AIP | Journal of Applied Physics

Nonlinear viscoelasticity of freestanding and polymer-anchored vertically aligned carbon nanotube foams

Ludovica Lattanzi, Jordan R. Raney, Luigi De Nardo, Abha Misra, and Chiara Daraio

Citation: J. Appl. Phys. **111**, 074314 (2012); doi: 10.1063/1.3699184
View online: http://dx.doi.org/10.1063/1.3699184
View Table of Contents: http://jap.aip.org/resource/1/JAPIAU/v111/i7
Published by the American Institute of Physics.

Nonlinear viscoelasticity of freestanding and polymer-anchored vertically aligned carbon nanotube foams

Ludovica Lattanzi,[1,2] Jordan R. Raney,[3] Luigi De Nardo,[1,2] Abha Misra,[4] and Chiara Daraio[5,6,a)]

[1]*Department of Chemistry, Materials, and Chemical Engineering "G. Natta," Politecnico di Milano, 20131 Milano, Italia*
[2]*INSTM, Consorzio Nazionale di scienza e tecnologia dei materiali, 50121 Firenze, Italia*
[3]*Materials Science, California Institute of Technology, Pasadena, California 91125, USA*
[4]*Instrumentation and Applied Physics, Indian Institute of Science, 560012 Bangalore, India*
[5]*Graduate Aerospace Laboratories (GALCIT), California Institute of Technology, Pasadena, California 91125, USA*
[6]*Applied Physics, California Institute of Technology, Pasadena, California 91125, USA*

(Received 7 July 2011; accepted 1 March 2012; published online 10 April 2012)

Vertical arrays of carbon nanotubes (VACNTs) show unique mechanical behavior in compression, with a highly nonlinear response similar to that of open cell foams and the ability to recover large deformations. Here, we study the viscoelastic response of both freestanding VACNT arrays and sandwich structures composed of a VACNT array partially embedded between two layers of poly(dimethylsiloxane) (PDMS) and bucky paper. The VACNTs tested are ~2 mm thick foams grown via an injection chemical vapor deposition method. Both freestanding and sandwich structures exhibit a time-dependent behavior under compression. A power-law function of time is used to describe the main features observed in creep and stress-relaxation tests. The power-law exponents show nonlinear viscoelastic behavior in which the rate of creep is dependent upon the stress level and the rate of stress relaxation is dependent upon the strain level. The results show a marginal effect of the thin PDMS/bucky paper layers on the viscoelastic responses. At high strain levels ($\varepsilon = 0.8$), the peak stress for the anchored CNTs reaches ~45 MPa, whereas it is only ~15 MPa for freestanding CNTs, suggesting a large effect of PDMS on the structural response of the sandwich structures. © *2012 American Institute of Physics*. [http://dx.doi.org/10.1063/1.3699184]

I. INTRODUCTION

Carbon nanotubes (CNTs) have been widely studied because of their excellent thermal,[1] electronic,[2] and mechanical[3,4] properties. Macroscopic stand-alone structures comprising CNTs have been fabricated as new materials with unique properties. Examples include 1D flexible yarns,[5,6] 2D sheets,[7] 3D "mats" or "forests" of aligned CNTs,[8–10] and disordered structures.[11] These systems have been suggested for several applications, including electronic[11,12] and field emission devices,[13] composites,[14,15] and bioactive materials.[16,17]

The partial anchoring of vertical arrays of carbon nanotubes (VACNTs) in a single, thin polymer film has been previously reported,[18,19] and the mechanical response of anchored VACNTs has been characterized under quasi-static compressive loading.[19] Anchored VACNTs have been shown to behave as excellent light-weight energy absorbing systems.[19] The development of nanocomposites based on VACNTs fully embedded in polymer and the effect of CNT morphology on the mechanical and electrical responses have been also studied.[20,21] It was shown that controlling the nanostructure morphology (e.g., the alignment, volume fraction, and length of CNTs) might enhance the nanocomposite response.

Freestanding VACNTs have been shown to behave like super-compressible foams, with a constitutive relation characterized by two distinct paths for loading and unloading, resulting in a hysteretic response.[22] Under cyclic compressive load, they have been reported to exhibit preconditioning effects and no fatigue failure, even with high strain amplitudes ($\varepsilon = \sim 0.6$) and a large number of cycles (5×10^5).[23] The micro- and nano-scale time-dependent mechanical response of freestanding VACNTs has been characterized using indentation techniques.[24–26] Under a spherical indenter, VACNT forests have been shown to undergo time-dependent creep deformation[26] and viscoelastic relaxation due to the thermally activated change in nanotube contacts.[24] Dense CNT brushes have been shown to exhibit a viscoelastic response under dynamic indentation with loads below the critical CNT buckling load.[25] Zhang *et al.*[26] have shown a dependence of the strain rate on the density of VACNT forests, reporting a lower creep deformation in denser material.

Here, we describe the bulk time-dependent response of millimeter-long VACNT arrays, both freestanding and polymer-anchored (sandwich structures). We performed bulk creep and stress-relaxation tests and fit the results using a time power-law. We tested the viscoelastic responses of all samples at different strain and stress levels in order to understand the bulk behavior of the VACNTs and the effects of polymer layers on the response of the sandwich structures.

a)Author to whom correspondence should be addressed. Electronic mail: daraio@caltech.edu.

II. MATERIALS AND METHODS

Arrays of CNTs (Fig. 1(a)) were grown in a chemical vapor deposition (CVD) reactor comprising liquid and gas injectors, as reported in Ref. 19. Toluene (C_7H_8) served as the carbon source. A feeding solution of ferrocene ($C_{10}H_{10}Fe$) in toluene [w/v] = 20 g l^{-1} was injected into the CVD reaction tube (T = 1098 K) at a rate of approximately 1 ml min^{-1} and was carried by argon carrier gas. Inside the tube, a constant Ar flow of 800 SCCM (SCCM denotes cubic centimeters per minute at standard temperature and pressure) was maintained at atmospheric pressure throughout the entire process. After growth, the CNT arrays were cooled to ambient temperature, and they were manually separated from their silicon oxide supporting substrate with a razor blade and cut into specimens with a cross sectional area of about 15 to 26 mm^2. The total thickness of the specimens was about 2 mm (corresponding to the CNT growth height), with a CNT outer diameter of ~46 nm and an array density range of 0.17–0.25 g cm^{-3}.[27] The orientation and alignment of CNT arrays of this type have been examined thoroughly in the past and have been found to vary along the height of the structure.[28] The volume fraction of the as-grown forests has also been characterized previously and was found to be ~10% to 15%.[22]

One set of specimens was sandwiched between two thin poly(dimethylsiloxane) (PDMS) films and bucky paper,[29] as shown in Fig. 1(b). Though the PDMS layers enhance the structural stability of the CNT arrays,[19] they also act as electrically insulating layers, preventing the use of CNT arrays in some of their potential multifunctional applications.[29] The insertion of bucky paper has been shown to restore electrical conductivity across the structure while maintaining the mechanical enhancement that arises from the PDMS, allowing the structures to be used for strain sensing and the monitoring of microstructural rearrangement.[29] To create the sandwich structures, we followed a multi-step process: first a thin layer of PDMS (~50 μm thick) was obtained by spin-coating uncured PDMS on a glass slide at 800 rpm. Then a film of bucky paper was placed on top of the PDMS, and the assembly was cured at 350 K for 1 h on a hot plate. A second layer of monomer PDMS was spun on top of the previously cured bucky paper/PDMS. The VACNTs were then pressed onto the polymer/bucky paper surface, and the assembly was heated at 350 K for 1 h, after which the cured film with the anchored CNTs was peeled off the glass slide. The process was then repeated to anchor the other side of the VACNTs. Bucky paper was obtained via the negative filtration of a 1.1 g l^{-1} CNT suspension in an isopropyl alcohol/water solution ([v/v] = 25%) that had been ultrasonicated overnight.

The samples were tested in compression using a electrodynamic materials testing machine (Instron E3000 system) at room temperature. A pre-load of 0.5 N was applied to all samples in order to provide uniform contact between the sample's surfaces and the compression platens, and to prevent slipping. Viscoelasticity was studied via stress-relaxation and creep tests; the engineering stress (σ) and strain (ε) were calculated as a function of time as

$$\sigma(t) = \frac{|F(t)|}{A_0}, \tag{1}$$

$$\varepsilon(\mathrm{t}) = \frac{L_0 - L(t)}{L_0}, \tag{2}$$

in which $F(t)$ is the measured force at time t (positive in compression), A_0 is the cross sectional area at time 0, L is the specimen height at time t, and L_0 is the original length at time 0.

For the stress-relaxation tests, strains of ε = 0.1, 0.2, 0.4, 0.6, and 0.8 were applied at a strain rate of 0.03 s^{-1} and maintained for 3×10^4 s. Creep tests were performed using stress values of 1, 4, 8, 12, 15, and 18 MPa that were initially applied at a stress rate of 1 MPa s^{-1} and maintained for 3×10^4 s.

Statistical analyses (normal probability test and analysis of variance [ANOVA] tests) were performed in order to

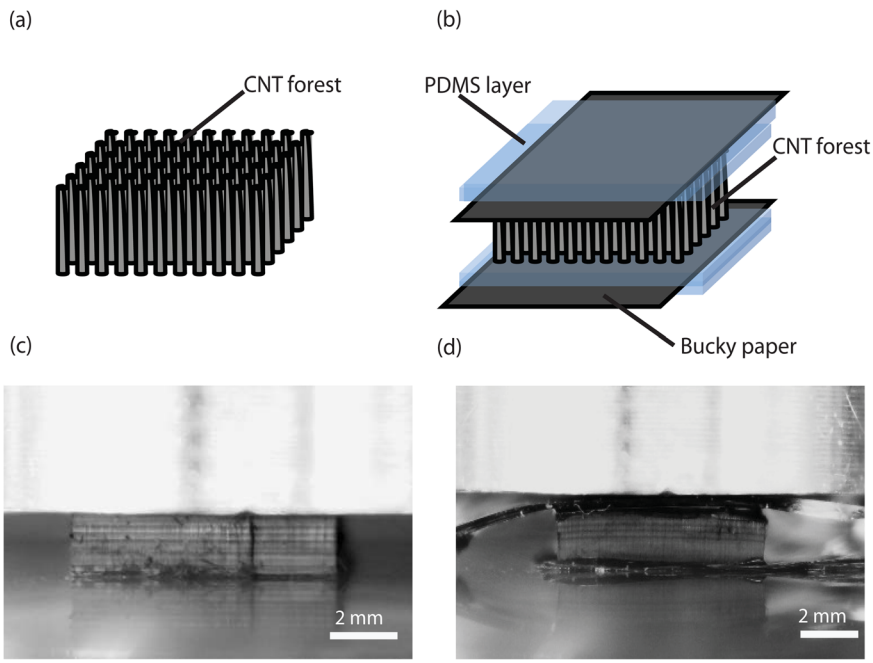

FIG. 1. Schematic diagram of (a) freestanding and (b) double-anchored CNT forests. Optical micrographs of (c) freestanding and (d) double-anchored CNT forests.

determine the dependence of the creep/relaxation rate on stress/strain, with the null hypothesis that no association existed between the rate and the stress/strain.

III. RESULTS AND DISCUSSION

In order to evaluate the influence of the polymer layer on the macroscopic mechanical response of the structure, we first performed quasi-static compressive tests by loading the specimens parallel to the CNT growth direction (along the CNT length) to the highest strain value ($\varepsilon = 0.8$) at a strain rate of 0.03 s^{-1}. The experimental setup is shown in Figs. 1(c) and 1(d). Both freestanding and sandwiched CNT forests were subjected to repeated compressive strains (100 cycles). All samples showed a stress-strain response characterized by hysteresis loops and exhibited stress softening (see Supplementary Material[37]). Both the freestanding and the polymer-anchored samples also showed the typical three-regime deformation response observed previously in freestanding VACNTs (e.g., Ref. 22): a short elastic region at low strain levels, followed by an extended plateau region, and finally a rapid increase of stress indicating the onset of densification. The freestanding and polymer-anchored VACNTs showed no significant differences in terms of the measured peak stress values or energy absorption. All quasi-static compression results obtained agree well with data previously reported for freestanding VACNTs.[19,22,23]

The macroscopic time-dependent behavior of VACNTs was then evaluated via creep and stress-relaxation tests. The creep behavior of freestanding VACNTs is shown in Fig. 2(a), and that of the sandwich structures is shown in Fig. 2(b). The increase in foam deformation over time with a step constant load exhibits a short primary stage and a long secondary stage in which the strain rate is constant.

The results obtained from the stress-relaxation tests for freestanding samples are reported in Fig. 3(a), and in Fig. 3(b) we show those for the sandwiched VACNTs. All samples show a decrease in stress with time and an increase of stress values with increasing step strain levels. The relaxation curves show a difference between freestanding and sandwiched specimens at the highest strain level ($\varepsilon = 0.8$), reaching ~15 MPa and ~45 MPa stress peaks, respectively. The stress-relaxation results show that under compression, anchored CNTs exhibited a gradual stress increase until a strain value of ~0.75 was reached, and above that a sudden increase was observed.

The progressive deformation under step constant stress [Fig. 2] and the decrease in stress over time with a step constant strain [Fig. 3] confirm the time-dependent behavior typical of viscoelastic materials.[30] During compression, CNTs

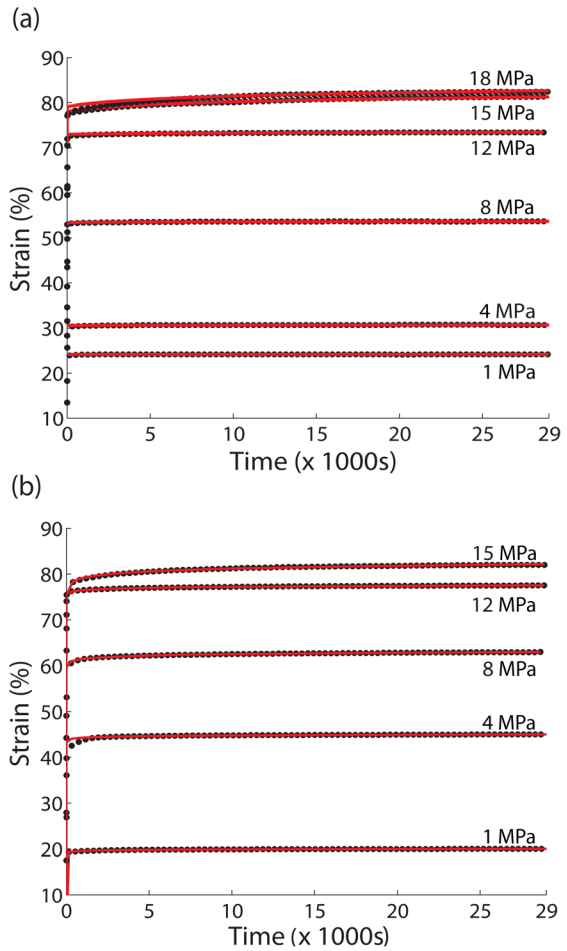

FIG. 2. Experimental creep response (points) and curve fitting (solid lines) of (a) freestanding and (b) double-anchored CNT forests.

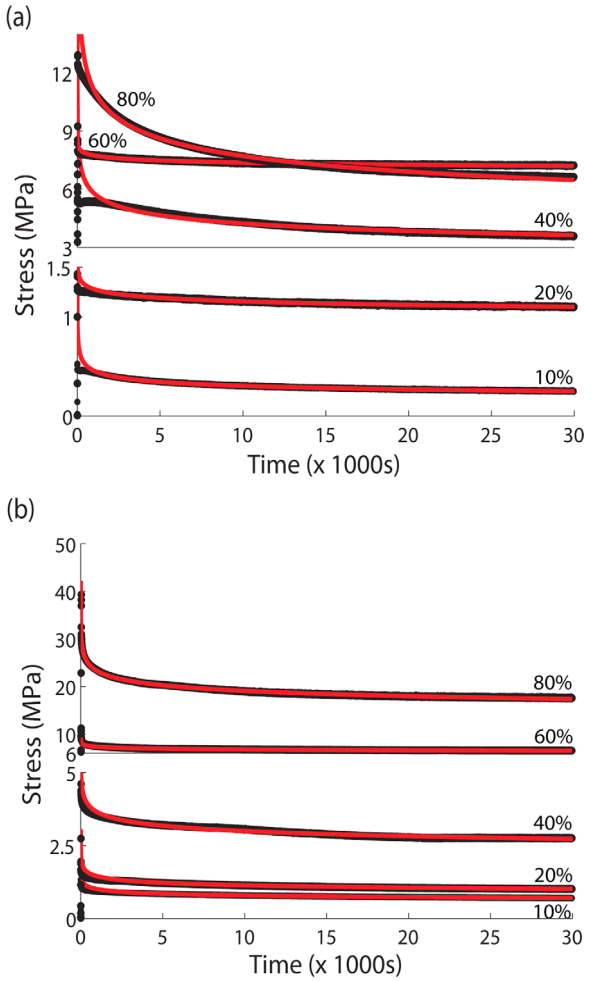

FIG. 3. Experimental stress-relaxation response (points) and curve fitting (solid lines) of (a) freestanding and (b) double-anchored CNT forests.

TABLE I. Creep exponent n (power-law exponent) for freestanding (n_F) and polymer-anchored (n_A) CNT forests. The table reports the values plotted in Figs. 4(a) and 4(b).

Stress (MPa)	1	4	8	12	15	18
n_F ($\times 10^{-3}$)	0	3.0 ± 1.7	2.8 ± 1.4	3.6 ± 1.1	10 ± 2.1	13.8 ± 3.1
n_A ($\times 10^{-3}$)	9.2 ± 3.7	4.0 ± 2.7	6.0 ± 1.7	4.9 ± 0.8	12.5 ± 1.5	…

change their alignment, becoming less oriented, breaking van der Waals forces, and creating new tube-tube interactions.[23] Such behavior can be compared to the conformational changes observed in polymer chains. The parallels between CNTs and polymers have been proposed by Green *et al.*, who explored the structure, properties, and rheology of CNTs, referring to the material as "the ultimate polymer."[31]

Despite the loss of alignment and the increase of adhesive interactions between nanotubes at high strains, the unloaded CNT arrays recovered their original height nearly in full, as has been observed previously.[22]

A more accurate description of the viscoelastic behavior can be obtained by studying the dependence of the relaxation rate on strain levels and of the creep rate on stress levels.[30] For linear viscoelastic materials, the relaxation/creep rate does not depend on the strain/stress level, and instead is characterized by a constant value. In contrast, nonlinear viscoelastic behavior is strongly dependent on the strain/stress level.[30] Many theories have been developed for the study of nonlinear viscoelasticity (e.g., Ref. 32). Because of the complexity of these nonlinear theoretical formulations, empirical approaches are often used[32] to describe the main features of the creep[30] and stress relaxation behavior[33] of viscoelastic materials. Here we use power functions of time to fit the creep (3) and stress relaxation (4) tests.

$$\varepsilon(t) = K_{cr} t^n, \tag{3}$$

$$\sigma(t) = K_{sr} t^m, \tag{4}$$

in which $\varepsilon(t)$ and $\sigma(t)$ are the strain and stress, respectively, as functions of time, and K_{cr} and K_{sr} are the power-law coefficients. The values n and m are dimensionless power-law exponents that indicate the rates of creep and stress relaxation, respectively.[33] Figures 2 and 3 show creep and stress-relaxation test results: the points represent the experimental data, and the solid lines represent the power function fit. The results confirm that the power-law gives a good representation of the creep and stress-relaxation behavior of both freestanding and sandwiched VACNTs. The values of the power-law exponents n and m are summarized in Tables I and II, respectively.

The creep exponent n varies as a function of applied stress, presenting three distinct regions [Fig. 4(a)]. At low stress values ($\sigma < 4$ MPa), freestanding CNTs show a near 0 creep exponent, suggesting the absence of secondary creep. At such low stress values, freestanding CNTs instantly deform and maintain the step strain for the entire 3×10^4 s. The absence of creep suggests that at low stress values, VACNTs do not show a viscoelastic response. The second region is characterized by a critical stress ($\sim$4 MPa) at which freestanding CNTs exhibit secondary creep showing a creep exponent of $\sim$0.005 and a viscoelastic response. The results suggest that until a certain stress of $\sim$12 MPa, n does not depend on the stress levels, showing the same value at each applied step stress (4, 8, and 12 MPa). The quasi-horizontal trend of n suggests an almost linear viscoelastic behavior of freestanding CNTs for stress in the 4–12 MPa range. In the third region (higher stress values [Fig. 4(a)]), the creep rate increases by nearly an order of magnitude, reaching values of 0.01 for 15 MPa and $\sim$0.015 for 18 MPa. The different creep exponent values observed in this third region suggest that the linear viscoelastic approach is valid up to a critical stress level, here $\sim$12 MPa, which is referred to as the linear viscoelastic threshold. Above this stress level, the response of the material becomes nonlinear.

The dependence of the creep rate on the applied step stress was also studied for the sandwiched VACNTs, as shown in Fig. 4(b), in order to understand the effect of PDMS layers on the macroscopic viscoelastic response. The results suggest that the polymer does not alter the main features observed for freestanding CNTs, showing comparable creep rates for step stress in the 4–12 MPa range and increased values of n for higher stress levels (15 MPa). At high enough stress levels (18 MPa), the sample loses its stability due to significant lateral deformation of the polymer layers.

An important difference between the creep responses of anchored and freestanding CNTs is observed at low stress values. At 1 MPa, the creep exponent n_A is greater than zero for polymer-anchored samples, reaching a value of $\sim$0.01, in contrast to the case of freestanding CNTs [Fig. 4(b) and Table I]. The presence of secondary creep at this stress level is probably due to the creep response of the polymer, which shows viscoelastic behavior even at low stress values. The creep rate of PDMS layers, tested separately, was in fact measured as $\sim$0.02 at 1 MPa, $\sim$0.03 at 4 MPa, and $\sim$0.06 at 8 MPa, showing appreciable nonlinearity.

Figure 4(c) shows the relaxation exponent (m) versus the strain for freestanding VACNTs, and Fig. 4(d) shows the same relation for sandwiched VACNTs. The results for

TABLE II. Relaxation exponent m (power-law exponent) for freestanding (m_F) and two side anchored (m_A) CNT forests. The table reports the values shown in Figs. 4(c) and 4(d).

Strain	0.05	0.1	0.2	0.4	0.6	0.8
m_F ($\times 10^{-2}$)	-16.0	-19.0 ± 2.8	-2.0 ± 1.7	-8.0 ± 1.7	-2.0 ± 0.58	-14.6 ± 1.1
m_A ($\times 10^{-2}$)	-5.7 ± 2.0	-7.0 ± 1.7	-9.6 ± 1.4	-6.7 ± 1.6	-5.0 ± 1.4	-7.9 ± 0.5

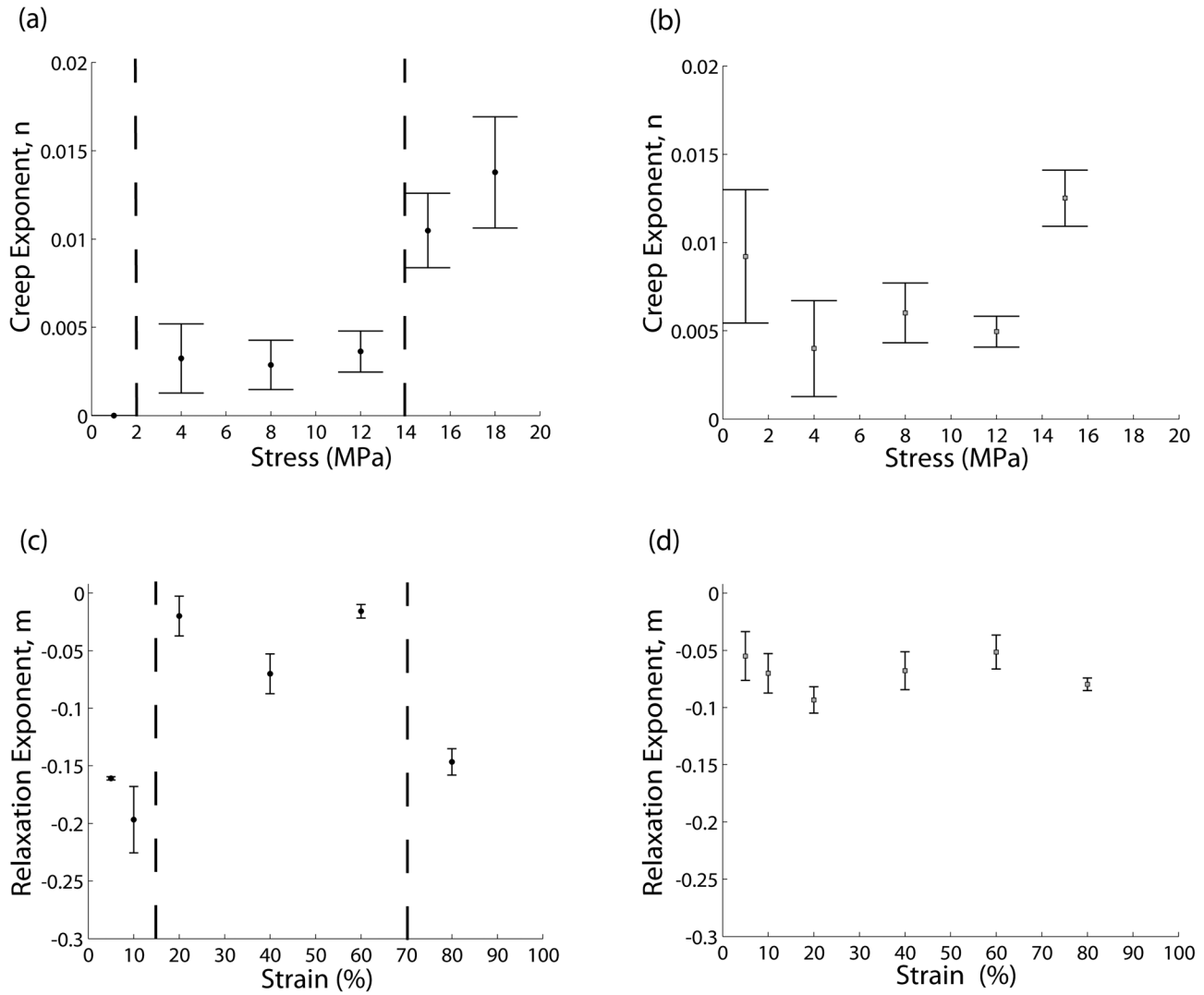

FIG. 4. Creep exponent n vs stress for (a) freestanding (n_F) and (b) double-anchored (n_A) CNT forests. Relaxation exponent m vs strain for (c) freestanding (m_F) and (d) double-anchored (m_A) CNT forests.

freestanding CNTs show again a response characterized by three different regions: an initial portion (up to $\varepsilon = 0.1$) characterized by a relaxation exponent of nearly -0.2; a second, from $\varepsilon = 0.2$ to $\varepsilon = 0.6$, in which the magnitude of m decreases by nearly an order of magnitude ($-0.05 < m < 0$); and finally an increase in the magnitude of the relaxation exponent for the applied step deformation $\varepsilon = 0.8$. Results show that at low strain values ($\varepsilon = 0.05$ and $\varepsilon = 0.1$), the viscoelastic response is significant, whereas at strain values ranging from $\varepsilon = 0.2$ to $\varepsilon = 0.6$, CNT forests do not show any appreciable viscoelasticity. The decrease in the magnitude of m is probably caused by the increased adhesive interactions between the nanotubes when they are squeezed together, as previously observed by Pathak *et al.*, who studied the viscoelasticity of dense carbon nanotube brushes by means of nanoindentation tests.[25] Pathak *et al.* explained such behavior by comparing CNT foams to polymers, like rubber, in which an increase in cross-linking leads to a decrease in the viscoelastic response. In contrast, the increased magnitude of m at $\varepsilon = 0.8$ is probably due to the development of cracks inside the VACNT arrays, causing a loss of interaction between adjacent nanotubes.

A different behavior is observed for the sandwich structures [Fig. 4(d)], in which the additional constraint due to the partial anchoring of the VACNTs in PDMS causes a decrease of the viscoelastic response at all strain levels and decreased nonlinearity in the rate of relaxation. If one compares the values of the relaxation and creep exponents, it is clear that relaxation proceeds faster than creep, confirming the nonlinear viscoelasticity of both freestanding and anchored CNTs.[34] Previous studies have demonstrated that nonlinearity causes relaxation to proceed more rapidly than creep.[34] In contrast, in a linear material, power-law creep and relaxation curves have the same slope.[34] In our study, the dependence of the relaxation/creep rate on the strain/stress was confirmed by statistical analysis. ANOVA tests performed on freestanding and anchored groups indicated that the creep rate n is strongly dependent upon stress for both freestanding ($p = 2.9 \times 10^{-6}$) and two side anchored ($p = 7.3 \times 10^{-3}$) CNTs. Similar results are also found for the relaxation rate ($p_F = 4.1 \times 10^{-6}$ and $p_A = 3.6 \times 10^{-2}$ for freestanding and sandwiched specimens, respectively), confirming the nonlinearity of the material.[33]

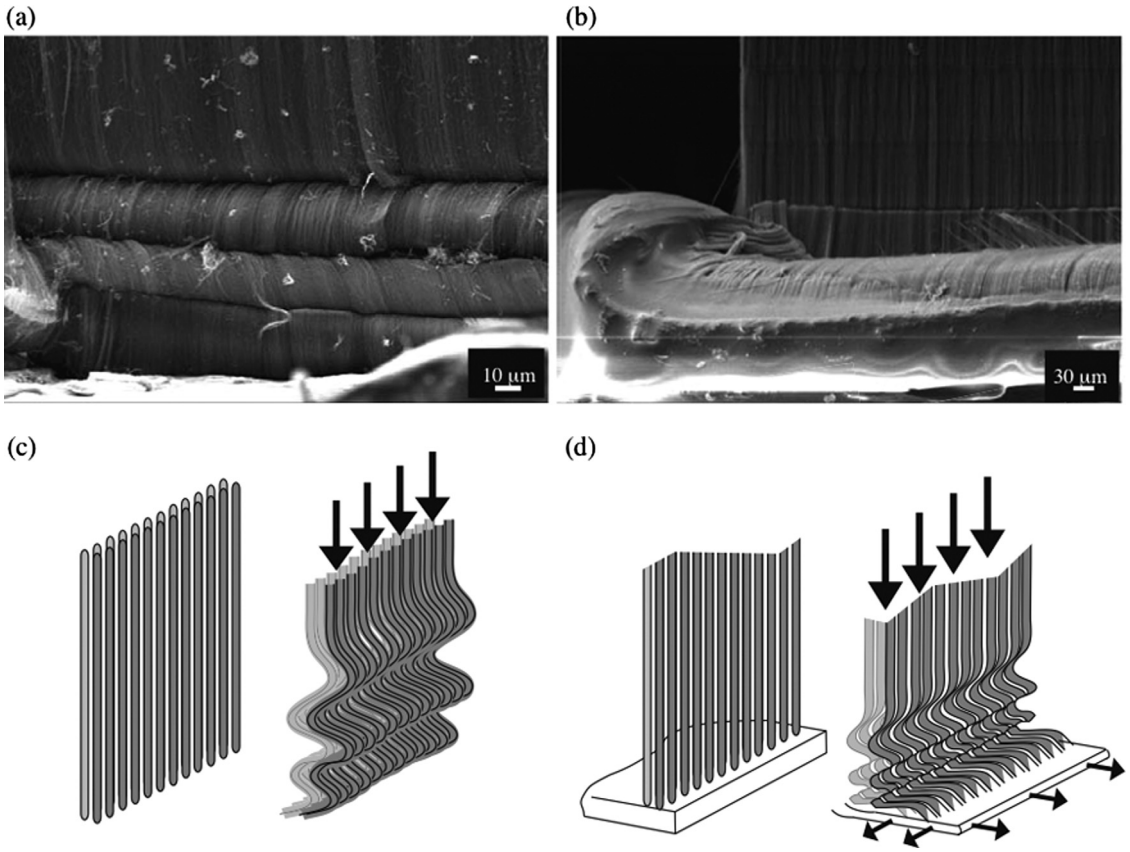

FIG. 5. Scanning electron microscope micrographs of the buckling area in the bottom section of (a) freestanding and (b) double-anchored CNT forests while compressed at $\varepsilon = 0.4$. Schematic illustration of the different buckling mechanisms in (c) freestanding and (d) double-anchored CNT forests.

The role of the polymer in the sandwich structures is relevant to the buckling mode and the stability of the material. Sandwich structures presented higher structural stability (for moderate strains) than did freestanding CNTs due to the different boundary conditions. We describe the deformation of freestanding and anchored CNTs with two different simple mechanical models using analogies with macroscopic column buckling. For freestanding samples, we consider both ends as pinned, with the CNT segments hinged by van der Walls forces.[35] For the anchored samples, we consider both ends as fixed. Referring to the formula derived by Euler,[36]

$$P_{cr} = \frac{\pi^2 EI}{(KL)^2}, \tag{5}$$

in which P_{cr} is the critical load, E is the modulus of elasticity, I is the area moment of inertia, K is the column effective length factor, and L is the unsupported length of the column. These simple assumptions result in a higher critical load for anchored CNTs because of the different column effective length factors ($K_F = 1$ for freestanding and $K_A = 0.5$ for sandwiched specimens).[36]

In order to evaluate the effects of PDMS on the buckling modes, we performed scanning electron microscope (SEM) analyses on both freestanding and anchored CNTs while the samples were compressed at a fixed strain value of ~0.4 using a controlled clamping mechanism. Figures 5(a) and 5(b) show the compression of freestanding and sandwiched CNTs, respectively. When uniaxially compressed, freestanding structures start to collapse with zig-zag buckles from the bottom [Figs. 5(a) and 5(c)], as was already observed by Cao *et al.*[22] In contrast, the sandwiched VACNTs buckle differently: the structure collapses by forming zigzag buckles that are then driven outward by the lateral deformation of the PDMS. This is evident in the SEM image in Fig. 5(b), and it is explained in the schematic diagram in Fig. 5(d). Such behavior might also explain why the strain of anchored CNTs is higher than the strain of freestanding CNTs for all the stress levels except for a stress value of 1 MPa. At low stress levels, the lateral deformation of the PDMS is minimal and therefore does not alter the CNT forest structure.

In order to quantify the effect of the polymer on the VACNTs, we calculated the ratio between the transverse (lateral) strain and the axial (longitudinal) strain at $\varepsilon = 0.6$. For freestanding and anchored CNTs, these values were ~0.01 and ~0.5, respectively.

IV. CONCLUSIONS

We studied the bulk viscoelastic response of millimeter-scale vertically aligned carbon nanotube arrays, both as freestanding material and in a sandwich structure, partially embedded between thin PDMS layers and bucky paper. The time-dependent behavior of these structures was characterized using stress-relaxation and creep tests. The stress-relaxation tests show a decrease in stress with time and an increase in stress values with increasing strain levels. The creep tests show two stages: a short primary stage and a long

secondary stage in which the strain rate is constant. Power functions of time were used to fit the stress-relaxation and creep curves in order to study the dependence of the relaxation/creep rate on strain/stress levels. The trend of the power-law exponents suggests that freestanding and anchored CNTs follow a nonlinear viscoelastic response. In freestanding CNTs, the trend of the creep exponent n shows that, initially, a linear viscoelastic response starts at a stress value of ~4 MPa, and it becomes nonlinear at the critical stress of ~12 MPa. In the sandwiched CNTs, the viscoelastic behavior begins at lower stress values (1 MPa) due to the viscoelasticity of the PDMS. The sandwiched CNTs, however, reached higher stress values at high strain levels ($\varepsilon = 0.8$) than did the freestanding material. The presence of polymer on the top and bottom surfaces of the samples affected the buckling behavior of the CNTs, resulting in zig-zag buckles driven outward by the lateral deformation of the polymer. The present study provides a detailed evaluation of the bulk time-dependent behavior of VACNTs as both stand-alone and polymer anchored sandwich structures. This understanding supports the use of bulk CNT-based structures as building blocks for high strength, low-density energy absorbing materials.

ACKNOWLEDGMENTS

L. De Nardo and L. Lattanzi acknowledge Regione Lombardia and INSTM for the project "Metahouse." J.R. Raney thanks the U.S. Department of Defense for support via a National Defense Science & Engineering Graduate (NDSEG) fellowship. This work is supported by the Institute for Collaborative Biotechnologies under Contract No. W911NF-09-D-0001 with the Army Research Office.

[1]P. Kim, L. Shi, A. Majumdar, and P. L. McEuen, Phys. Rev. Lett. **87**(21), 1–4 (2001).
[2]T. W. Ebbesen, H. J. Lezec, H. Hiura, J. W. Bennett, H. F. Ghaemi, and T. Thio, Nature **382**, 54–56 (1996).
[3]M. M. J. Treacy, T. W. Ebbesen, and J. M. Gibson, Nature **381**, 678–680 (1996).
[4]J. P. Lu, J. Phys. Chem. Solids **58**, 1649–1652 (1997).
[5]K. Jiang, Q. Li, and S. Fan, Nature **419**, 801 (2002).
[6]M. Zhang, K. R. Atkinson, and R. H. Baughman, Science **306**, 1358–1361 (2004).
[7]M. Zhang, S. Fang, A. A. Zakhidov, S. B. Lee, A. E. Aliev, C. D. Williams, K. R. Atkinson, and R. H. Baughman, Science **309**, 1215–1219 (2005).
[8]C. P. Deck, J. Flowers, G. S. B. McKee, and K. Vecchio, J. Appl. Phys. **101**, 023512 (2007).
[9]R. Andrews, D. Jacques, A. M. Rao, F. Derbyshire, D. Qian, X. Fan, E. C. Dickey, and J. Chen, Chem. Phys. Lett. **303**, 467–474 (1999).
[10]K. Hata, D. N. Futaba, K. Mizuno, T. Namai, M. Yumura, and S. Iijima, Science **306**, 1362–1364 (2004).
[11]C. Niu, E. K. Sickel, R. Hoch, D. Moy, and H. Tennent, Appl. Phys. Lett. **70**, 1480–1482 (1997).
[12]A. Najafabadi, S. Yasuda, K. Kobashi, T. Yamada, D. N. Futaba, H. Hatori, M. Yumura, S. Iijima, and K. Hata, Adv. Mater. **22**, E235–E241 (2010).
[13]S. S. Fan, M. G. Chaplind, N. R. Franklin, T. W. Tombler, A. M. Cassel, and H. Dai, Science **283**, 512–514 (1999).
[14]V. P. Veedu, A. Cao, X. Li, K. Ma, C. Soldano, S. Kar, P. M. Ajayan, and M. N. Ghasemi-Nejhad, Nature Mater. **5**, 457–462 (2006).
[15]P. M. Ajayan, L. S. Schadler, C. Giannaris, and A. Rubio, Adv. Mater. **12**, 750–753 (2000).
[16]W. Wei, A. Sethuraman, C. Jin, N. A. Monteiro-Riviere, and R. J. Narayan, J. Nanosci. Nanotechnol. **7**, 1284–1297 (2007).
[17]M. Meyyappan, *Carbon Nanotubes: Science and Application* (CRC Press, Boca Raton, FL, 2005).
[18]E. B. Sansom, D. Rinderknecht, and M. Gharib, Nanotechnology **19**, 1–6 (2008).
[19]A. Misra, J. R. Greer, and C. Daraio, Adv. Mater. **21**, 334–338 (2009).
[20]E. J. Garcia, B. L. Wardle, and A. J. Hart, Composites, Part A **39**, 1065–1070 (2008).
[21]H. Cebeci, R. G. de Villoria, A. J. Hart, and B. L. Wardle, Compos. Sci. Technol. **69**, 2649–2656 (2009).
[22]A. Cao, P. L. Dickrell, W. G. Sawyer, M. N. Ghasemi-Nejhad, and P. M. Ajayan, Science **310**, 1307–1310 (2005).
[23]J. Suhr, P. Victor, L. Ci, S. Sreekala, X. Zhang, O. Nalamasu, and P. M. Ajayan, Nat. Nanotechnol. **2**, 417–421 (2007).
[24]S. Dj. Mesarovic, C. M. McCarter, D. F. Bahr, H. Radhakrishnan, R. F. Richards, C. D. Richards, D. McClainb, and J. Jiao, Scr. Mater. **56**, 157–160 (2007).
[25]S. Pathak, Z. G. Cambaz, S. R. Kalidindi, J. G. Swadener, and Y. Gogotsi, Carbon **47**, 1969–1976 (2009).
[26]Q. Zhang, Y. C. Lu, F. Du, L. Dai, J. Baur, and D. C. Foster, J. Phys. D Appl. Phys. **43**, 315401 (2010).
[27]J. R. Raney, A. Misra, and C. Daraio, Carbon **49**, 3631–3638 (2011).
[28]M. Pinault, V. Pichot, H. Khodja, P. Launois, C. Reynaud, and M. M. L'Hermite, Nano Lett. **5**, 2394–2398 (2005).
[29]A. Misra, J. R. Raney, L. De Nardo, A. E. Craig, and C. Daraio, ACS Nano **5**, 7713–7721 (2011).
[30]W. N. Findley, J. S. Lai, and K. Onaran, *Creep and Relaxation of Nonlinear Viscoelastic Materials* (North-Holland, Amsterdam, 1976).
[31]M. J. Green, N. Behabtu, M. Pasquali, and W. W. Adams, Polymer **50**, 4979–4997 (2009).
[32]M. Hadid, S. Rechak, and A. Tati, Mater. Sci. Eng., A **385**, 54–58 (2004).
[33]P. Provenzano, R. Lakes, T. Keenan, and R. Vanderby, Ann. Biomed. Eng. **29**, 908–914 (2001).
[34]R. S. Lakes and R. Vanderby, J. Biomech. Eng. **121**, 612–615 (1999).
[35]A. A. Zbib, S. Dj. Mesarovic, E. T. Lilleodden, D. McClain, J. Jiao, and D. F. Bahr, Nanotechnology **19**, 7 (2008).
[36]Z. P. Bazant and L. Cedolin, *Stability of Structures* (Dover, New York, 2003).
[37]See supplementary material at http://dx.doi.org/10.1063/1.3699184 for the cyclic compressive quasi-static mechanical response of freestanding and double-anchored CNT forests.